Environ. Sci. Technol. **2005**, *39,* 206−212

Adsorption of Ethylene Glycol Vapor on α-Al_2O_3 (0001) and Amorphous SiO_2 Surfaces: Observation of Molecular Orientation and Surface Hydroxyl Groups as Sorption Sites

DINGFANG LIU, GANG MA, MAN XU, AND HEATHER C. ALLEN*
Department of Chemistry, The Ohio State University, 100 W. 18th Avenue, Columbus, Ohio 43210

Vapor adsorption is an important process influencing the migration and the fates of many organic pollutants in the environment. In this study, adsorption of ethylene glycol (EG) vapor onto single crystal α-Al_2O_3 (0001) and fused SiO_2 (amorphous) surfaces was studied with sum frequency generation spectroscopy, a well-suited surface specific technique for probing interfacial phenomena at the molecular scale. Air−aqueous EG solutions were also investigated to compare to the adsorption at the air−solid interface in the presence of water vapor. The gauche conformer of EG molecules dominates the air−aqueous EG solution interface, and EG molecules act as hydrogen acceptors at the air−liquid interface. Water and surface hydrophilic/hydrophobic properties play important roles for the adsorption of EG onto silica and alumina surfaces. The adsorbed EG molecules interact in different ways at the two different oxide surfaces. EG molecules weakly physisorb onto the α-Al_2O_3 (0001) surface by forming relatively weak hydrogen bonds with surface water molecules. On the silica surface, the suppression of the silanol OH stretching peak indicates that EG molecules form hydrogen bonds with silanol OH groups.

Introduction

Vapor adsorption onto oxide surfaces occurs in unsaturated soils and on mineral aerosols in the atmosphere. Vapor adsorption influences the contaminant migration and fate in the environment and can modify surface properties of the mineral particles, such as reactivity, hydrophobicity/hydrophilicity, and surface charge (*1*, *2*). In the troposphere, mineral aerosols can act as reactive surfaces with trace organic or inorganic atmospheric gases. The heterogeneous reactions between mineral aerosol and organic gases are critical for governing the trace atmospheric gas budget (such as O_3) (*3*, *4*). Among the metal oxides studied, silica and alumina are the most extensively studied because of their ubiquitous presence in soil and mineral aerosols (*3*−*5*).

It is well-known that the reactivity of silica and alumina surfaces is strongly influenced by the degree of surface hydroxylation. For example, small quantities of H_2O in chromatographic columns are known to have a large effect on the specificity of silica powders and surfaces to polar chemicals (*6*, *7*). Both silica and alumina surfaces are quickly hydroxylated after contact with water vapor, and hydration also modifies oxide surface structures. The hydrated oxide surface structure is not the perfect termination of the oxide bulk structure. The clean α-alumina (0001) surface is Al-terminated and is significantly relaxed relative to the bulk structure under ultrahigh vacuum (UHV) conditions, whereas the fully hydrated surface is oxygen terminated, and the surface structure is an intermediate between α-Al_2O_3 and γ-Al(OH) (*8*). Ab initio molecular dynamic calculations reveal that during the hydration, the coordinated unsaturated surface Al ions provide strong Lewis acid sites for H_2O adsorption, and dissociation of adsorbed H_2O generates two types of surface hydroxyl groups: $O_{ads}H$ and O_sH (O_{ads}, water oxygen; O_s, surface oxygen) (*9*). Numerous studies have been completed on the thermal stability of various types of hydroxyl groups on silica surfaces (*10*−*16*). Theoretical studies have found that the formation of a Si−OH group on quartz surfaces due to dissociative adsorption of water is preferred and causes a significant lowering of the surface energy (*17*). Under ambient conditions, many researchers have demonstrated that silica and alumina surfaces are covered with several monolayers of water molecules by forming hydrogen bonds either between surface hydroxyl and water molecules or between individual water molecules (*4*, *14*, *15*, *18*, *19*).

For adsorption of nonionic organic vapor on hydroxylated metal oxide surfaces, there are two main types of interaction forces: van der Waals (dispersion force) interaction being universal for many compounds and the interaction with formation of hydrogen bonds between the surface hydroxyl group and adsorbed molecules (*15*, *20*). Many IR studies have been dedicated to the investigation of hydrogen bonds of silanol groups upon adsorption. In addition, IR spectroscopy under various temperature conditions has been utilized to investigate the adsorption properties of organic compounds on oxide surfaces for various applications (*11*, *14*, *15*, *20*−*26*), where experiments were typically carried out in controlled environmental conditions such as vacuum, absence of water vapor after hydroxylation or hydration, etc. Based on hundreds of studies of organic adsorption on the silica surface, it has been concluded that hydrogen bond formation between electronegative atoms or π electrons of adsorbate molecules and the hydrogen atoms of the silanol groups plays a major role in adsorption of molecules from the vapor state (*15*, *20*).

The sorption of organic vapor to mineral oxide surfaces under ambient environmental conditions has been shown to follow these mechanisms (*27*, *28*): (1) Organic vapor adsorbed to the mineral oxide surface. The organic vapor can be physically adsorbed and/or reacted with the surface aluminol or silanol group. (2) Organic vapor adsorbed within/on the surface water film that is adsorbed on the mineral surface. (3) Organic vapors are solvated into the adsorbed water layers (a quasi-liquid water layer). Using gas chromatographic methods, Goss et al. (*27*−*31*) measured surface−air adsorption constants of a diverse set of 50 organic vapors on silica and alumina surfaces at different relative humidities (RH) and found that, comparing with the adsorption constants at different relative humidities, adsorbed water on the oxide surface plays a crucial role on the organic adsorption behavior. Mechanism 1 only occurs on surfaces that were not completely covered with water (*28*). With complete water layer coverage, mechanism 2 dominates for all the organics studied except for polar molecules such as methanol or small organic acids (*28*, *29*). At very high water relative humidities (90−100%), an increase of adsorption was observed, and it was speculated that this is due to a change in the orientation

* Corresponding author e-mail: allen@chemistry.ohio-state.edu.

10.1021/es049066a CCC: $30.25
Published on Web 11/18/2004

of the water molecules that form the surface water layer to which the organic adsorbs (*27*). When the quantity of water on the mineral oxide surface reaches a value between 4 and 5 monolayers, Henry's law can be applied to quantify the organic vapor retention (*32*, *33*). While these studies provide useful information by quantifying the vapor surface adsorption at different relative humidities, additional research is needed to fully understand the adsorption mechanisms at the air−solid interface. A surface-selective technique with the capability of molecular level resolution would be useful to provide support for the theories postulated from the macroscopic experimental results. In this study, a surface-selective spectroscopic technique, sum frequency generation (SFG) vibrational spectroscopy, was used to investigate ethylene glycol vapor adsorption on single crystal α-alumina (0001) and fused silica surfaces. SFG spectra can provide molecular-level information of adsorption at the air−solid interface.

Surface Specific Probing Techniques. For the introduction of surface specific probing techniques, there are several excellent detailed reviews by Al-Abadleh and Grassian (*4*), Brown and Sturchio (*34*), and Brown et al. (*35*). These reviews not only summarize surface sensitive techniques but also provide both introductory and the latest research updates on the metal oxide surface. The theory of SFG can be found in other publications (*36*−*40*). Here, a brief introduction of sum frequency generation spectroscopy is provided since it is the focus of this study.

SFG is a second-order nonlinear process that occurs in noncentrosymmetric environments such as at interfaces including the air−solid interface under the electric-dipole approximation. The SFG intensity, I_{SFG}, as shown in eq 1

$$I_{SFG} \propto |\chi^{(2)}|^2 = |\chi^{(2)}_{NR} + \sum_{\upsilon} \chi^{(2)}_{\upsilon}|^2 \qquad (1)$$

is proportional to the absolute square of the macroscopic second-order nonlinear susceptibility, $\chi^{(2)}$, which consists of resonant terms ($\chi^{(2)}_{\upsilon}$) and a nonresonant term ($\chi^{(2)}_{NR}$). When the frequency of an incident infrared beam, ω_{IR}, is resonant with a vibrational mode of an interfacial molecule, υ, the resonant susceptibility term $\chi_{\upsilon}{}^{(2)}$ dominates $\chi^{(2)}$ and a SFG intensity enhancement is observed. $\chi^{(2)}_{\upsilon}$ is shown in eq 2

$$\chi^{(2)}_{\upsilon} \propto \frac{A_{\upsilon}}{\omega_{\upsilon} - \omega_{IR} - i\Gamma_{\upsilon}} \qquad (2)$$

where A_{υ} is the amplitude of the transition moment, ω_{υ} is the frequency of the transition moment, and Γ_{υ} describes the line-width of the transition. The amplitude, A_{υ}, is nonzero when the Raman and the infrared transitions are spectroscopically allowed.

Experiment and Chemicals

Sum Frequency Generation. In the Allen Lab, two types of SFG systems are available. One is a broad bandwidth SFG (BBSFG) system, and the other is a scanning SFG system. In this study, the scanning SFG system was used to investigate both the C−H stretching region and the broad hydrogen bonding region at the oxide surfaces. A brief description of the scanning SFG system is given below.

The scanning SFG system utilizes a visible beam at 532 nm and an infrared beam tunable from 2500 to 4000 cm^{-1} with a bandwidth of ~4−8 cm^{-1} depending on the spectral region. The 532 nm beam is generated by doubling the frequency (second harmonic) of the 1064 nm pump source from an EKSPLA PL 2143A/SS Nd:YAG laser (29 ps pulse duration and 10 Hz repetition rate). The infrared beam is generated from a KTP−KTA based optical parametric generator/amplifier (OPG/OPA) system (LaserVision). The input 532 nm intensity is focused using a plano-convex lens (CVI Laser, 500 mm focal length) and is placed ~490 mm before the sample surface to provide a ~1 mm beam diameter and 400 μJ per pulse of 532 nm light on the sample surface. The infrared is focused at the sample surface using a BaF_2 lens (200 mm focal length), where it has < 0.5 mm beam diameter, and is ~300−650 μJ per pulse depending on the spectral region. This IR profile is shown in Figure 1. The input angles are ~45° and ~53° from the surface normal for the 532 nm and infrared beams, respectively. The detection angle is set to 45.6° from the surface normal for sum frequency detection. Several spatial, Schott glass and notch filters are used to block the 532 nm beam from entering the detection system. A 512 × 512 pixel array, 12.3 mm × 12.3 mm active area, 24-micron square pixel size, back illuminated CCD (DV412, Andor Technology) is used to detect the sum frequency signal. The CCD is thermoelectrically cooled, and the CCD temperature was set at −45 °C during the experiments. A home-written program in Labview and C+ languages was used for data acquisition. The scanning SFG spectra presented in this paper were acquired using a 10 or 30 s exposure time for each data point, and spectra were acquired anywhere from 20 to 50 min (from 2700 to 4000 cm^{-1}). The spectra presented here are the average to at least two replicate spectra. The polarization combination used for the scanning SFG experiments presented here is S, S, and P for the SFG, 532 nm, and infrared beams, respectively. The nonresonant response from the GaAs surface is shown in Figure 1 and can be used for normalization; however, in the experiments presented here, spectra were normalized to the incident IR energy also shown in Figure 1 since we obtain these data in real time. The spectra were acquired at the ambient condition of 23 °C and ~50% RH.

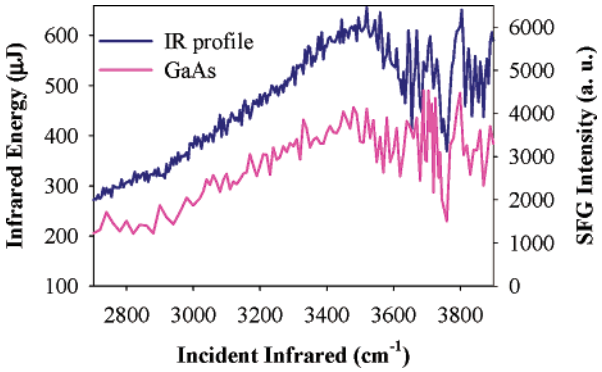

FIGURE 1. The infrared energy profile and the nonresonant sum frequency generation response from a GaAs surface.

Materials and Chemicals

The α-Al_2O_3 single crystal (c-cut, (0001) plane) parallel plates were purchased from Marketech International with a purity of >99.995%. The crystal was highly polished with a surface quality of 20−10 (alumina crystals without a highly polished surface can generate white-light in the bulk more efficiently and also produce lower signal intensities). The infrared grade fused silica plates were purchased from Quartz Plus Inc. According to the manufacturer data, the surface quality is 60−40, flatness ≅ 5 waves, parallelism < 15′, surface roughness = 1.5−3 nm, and bulk hydroxyl content ≤ 8 ppm. The alumina crystals were investigated by XPS after being received from the supplier to make certain that there was no inorganic contamination (especially silica) at the alumina surface. Before the SFG experiments, the oxides were annealed in a muffle oven (Fisher Scientific, Isotemp Muffle Furnace) at 900 °C for more than 12 h in order to remove possible organic contamination. After the crystal was cooled

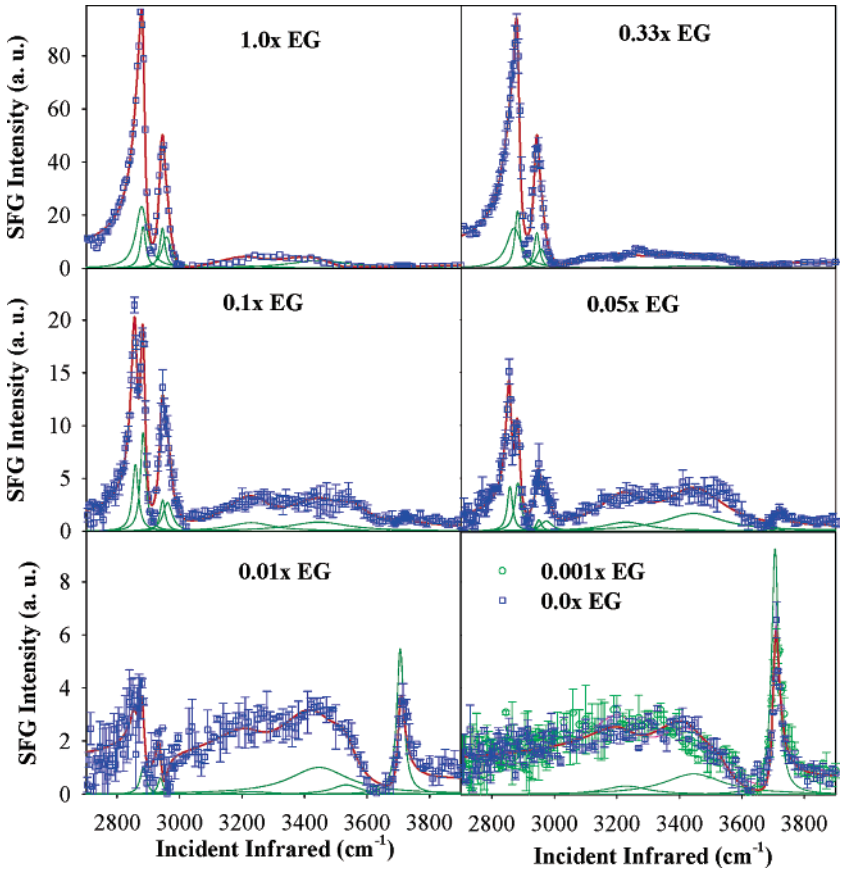

FIGURE 2. Sum frequency generation spectra of aqueous ethylene glycol solutions. Red lines are spectroscopic fits, and dark green lines are component peaks. Each spectrum shown is the average of at least 2 replicates except for neat ethylene glycol, and error bars are the standard deviations of the replicates.

to room temperature, the crystal was kept under ambient conditions for more than 30 min to allow equilibrium with the water vapor in the air. Then, the SFG experiments were performed on the alumina surface before and after the ethylene glycol adsorption.

The adsorption experiments were completed by placing the oxide into a sealed glass container with ~0.1 Torr partial pressure of ethylene glycol vapor under ambient conditions (1 atm pressure at 23 ± 1 °C). After 2 h exposure, oxide plates were purged with organic free air for 30 min. The oxide plates were then placed back onto the sample stage to investigate the air−solid interface by SFG spectroscopy.

Anhydrous ethylene glycol (99.8%) was purchased from Aldrich Chemicals and used as received. Deionized water was obtained from a Millipore Nanopure system (18.3 MΩ·cm). The relative humidity measurement was carried out by using a digital hygrometer/thermometer (Traceable, Control Company) with an accuracy of ±2% for relative humidity and ±1 °C for temperature.

Curve-Fitting of the SFG Spectra. Since an SFG-active vibrational mode must be both IR-active and Raman-active, an IR spectrum and a Raman spectrum of the chemicals of interest were obtained and analyzed before performing the SFG spectrum curve-fit. By performing curve-fits on the IR and Raman spectra, the number of peaks, peak position, and bandwidth of the both Raman- and IR-active modes can be obtained. These peak parameters are used as references when setting the initial guess and the confinement parameters in the SFG curve-fitting process as well as determining the possible numbers of the peaks that can exist in the SFG spectrum. In the Raman and IR fitting, the intensity is the summation of each vibration's intensity, whereas in SFG the intensity is the absolute square of the summation of each vibration's $\chi_v^{(2)}$ and $\chi_{NR}^{(2)}$ as shown in eq 1. This leads to different spectral character for SFG spectra relative to Raman and IR spectra because the relative phase of the SFG response for each overlapping vibrational mode can have a profound effect on the shape of the resultant SFG spectra. Therefore, SFG spectra interpretation must occur after deconvolution into the component peaks since direct comparison of SFG spectra to Raman and IR spectra may be misleading. In addition to the inclusion of phase, different nonresonant parameters were used to fit the SFG spectra. This parameter varied substantially for the air−liquid versus the different air−solid interfaces.

Results and Discussion

Ethylene Glycol at Air−Liquid Interfaces. Sum frequency generation spectra of aqueous ethylene glycol solutions are shown in Figure 2. The spectra cover both the CH (2700−3000 cm^{-1}) and OH (3000−3900 cm^{-1}) stretching regions and were collected using the $S_{SFG}S_{Vis}P_{IR}$ polarization configuration (the electric field vector for the S polarization is perpendicular to the incident plane, and for P polarization, it is parallel to the incident plane). In the CH stretching region, the peak around 2875 cm^{-1} is attributed to the CH_2 symmetric stretching (SS) modes. There is some controversy on the assignment of the smaller peak observed at ~2940 cm^{-1}, some follow general IR and Raman assignments by assigning it to the CH_2 asymmetric stretching (AS) modes (*41*), and recent SFG work assigns it to the Fermi resonance of the overtone of the CH_2 bending mode with the fundamental of SS modes by comparing the SFG intensity of EG at different polarization configurations (*42*). We assign the peak at ~2940 cm^{-1} to CH_2−AS modes as discussed below.

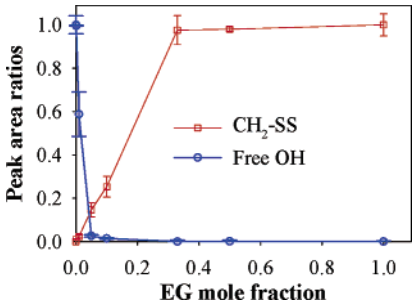

FIGURE 3. Peak area ratios of CH_2−SS and free OH stretching of surface water change with the concentration of ethylene glycol in aqueous solutions. The peak areas of the CH_2−SS are the total area for two fitted component bands. One fitted free OH peak centered at ~3700 cm^{-1} accounts for the area of the water free OH peak. The ratios are relative to neat ethylene glycol for the CH_2−SS and to neat water for the free OH.

The SFG intensity in the CH stretching region of aqueous ethylene glycol solutions increases with the concentration of the ethylene glycol in the solution, as one would expect. However, the CH_2−SS peak is split into two prominent peaks at concentrations ≤ 0.1 mole fraction EG, suggesting that there are at least two components to the CH_2−SS. The splitting is not observed in Raman and IR spectra of the bulk solutions confirming that the distribution of bulk and surface EG−water complexes are different. The splitting observed in our SFG surface spectra suggests that there is a critical H_2O concentration needed to organize the EG molecules into fewer, but more highly probable, EG conformers at the solution surface. One can view this as a surface solvation effect since the addition of solvent water molecules gives rise to the stabilization of fewer EG conformers at the solution surface. Hydrogen bonding between water and EG molecules plays a key role in the stabilization of fewer conformers at the surface, whereas in the bulk, solvation is 3-dimensional and therefore different. (Gas-phase cluster data on EG−water complexes is helpful to explain the EG−water interactions (*41*).) The splitting of the CH_2−SS peak also indicates that the peak at ~2940 cm^{-1} can be attributed to CH_2−AS modes, otherwise a similar splitting feature would have been observed if this peak is due to Fermi resonance modes.

Various ab initio calculations in gas and condensed phases reveal that the gauche conformer dominates the EG populations (*41*, *43*−*45*). Since the trans conformer is internally centrosymmetric, one would expect minimal if any SFG intensity according to the spectroscopic rules for SFG (*46*). However, a strong methylene SFG response is observed as shown in Figure 2 indicating that at the air−liquid interface EG gauche conformers are also dominant, consistent with these previous calculations.

The hydrogen bonded OH stretches are clearly observed in the 3000−3600 cm^{-1} region; however, free OH stretches of EG (3600−3800 cm^{-1} region (*47*, *48*)) are not observed for the neat EG−air spectrum. This indicates that, unlike water molecules with about 20% of OH dangling freely at the air−liquid interface (*49*), the diols of the EG molecules are hydrogen bonded at the interface. This leaves hydrophobic alkyl groups pointing from the liquid surface into the air phase and indicates that EG at its air−liquid interface behaves orientationally similar to methanol and ethanol (*50*, *51*).

The free OH stretching (3700 cm^{-1}) of water molecules nearly disappears at concentrations ≥ 0.1x EG, and only shows a weak response in the 0.05x EG solution as shown in Figure 2. This indicates that the EG molecules at the air−liquid interface are hydrogen acceptors (in addition to being hydrogen donors) in the EG−water binary system. That is, the oxygens of the EG diols are hydrogen bonding to the hydrogens of the dangling (free) OH of surface water. Figure 3 summarizes the peak intensities for both the CH_2−SS for

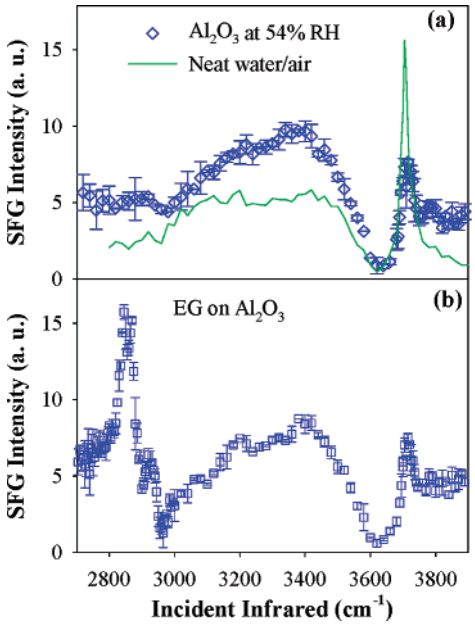

FIGURE 4. Sum frequency generation spectra of (a) the α-Al_2O_3 (0001) surface before and (b) after exposure to ethylene glycol vapor at 54% RH. The neat water sum frequency spectrum acquired using the same setup is plotted for comparison.

EG and the free OH for water (relative ratios to neat EG for CH_2−SS and to neat water for free OH). The free OH intensity decreases substantially from 0.001x to 0.05x EG solution (1 EG:19 H_2O: ~4 dangling OH). There are two factors that need to be considered when the SFG intensity is used for the quantitative spectral analysis. The first factor is the increased surface number density of EG molecules relative to the bulk concentration (*41*) since EG slightly partitions to the surface of its aqueous solution (decreasing surface tension with increasing EG concentrations). The second factor is the nature of SFG (SFG intensity depends on both the interfacial number density and the orientation of these molecules). However, the steep drop of the free OH intensity at such a low EG concentration strongly suggests that EG has a propensity for forming hydrogen bonds with the dangling OH (H-donor) of water at the interface. These findings are consistent with previous studies on aqueous methanol solutions, also an alcohol, which indicated that methanol is a more efficient hydrogen-bonding acceptor when it resides in the interfacial region (*51*).

Ethylene Glycol at Air−Solid Interfaces. The SFG spectra of α-Al_2O_3 (0001) at 54% relative humidity before (clean) and after exposure to EG vapor are shown in Figure 4. A neat water spectrum acquired using the same parameters (IR and 532 nm energy, exposure time etc.) is also plotted for comparison. The spectrum of clean α-alumina (0001) shows intensity in the hydrogen bonded OH stretching region (3000−3600 cm^{-1}), consistent with infrared studies of water adsorption at the α-Al_2O_3 (0001) surface (*9*, *18*). Recently, Al-Abadleh and Grassian studied surfaces of both single crystal and particles of α-alumina under 1 to 95% RH conditions using FT-IR spectroscopy (*18*). They found that water adsorbs on the surface in an ordered fashion with the formation of a stable hydroxide layer below ~10% RH, and water molecules form a structured overlayer between 10 and 70% RH. A quasi-liquid layer was also indicated to form on the surface above 70% RH. According to Al-Abadleh and Grassian, there are ~3 monolayers of water molecules formed on the α-alumina (0001) surface at 54% RH. At 296 K and 54% RH, our SFG spectra suggest that the α-alumina (0001) surface is hydrated with the possibility of several monolayers of water molecules, generally consistent with previous IR studies (*9*, *18*). Yet, in the free OH region of Figure 4, a

relatively sharp peak is observed at ~3710 cm^{-1}. In this region, both the free OH stretching of adsorbed water molecules and the free aluminol OH stretching can contribute to the SFG response. (The vibrational frequency of the aluminol OH stretch with the oxygen coordinated by three aluminum atoms has been previously observed at ~3710 cm^{-1} by using infrared absorption spectrocopy (*52*, *53*).) At relatively high RHs, there is still a possibility of isolated aluminol hydroxyl groups existing on the alumina surface (*18*, *54*) even though most of the hydroxyl groups have formed hydrogen bonds with adsorbed water molecules.

Since the refraction index of α-Al_2O_3 ($n_s \approx 1.77$) is larger than that of neat water ($n_s \approx 1.33$) and SiO_2 ($n_s \approx 1.46$), there should be less SFG signal reflected from the alumina surface according to nonlinear Fresnel coefficient calculations, and yet an enhanced SFG signal intensity is observed in this spectral region for the alumina surface relative to the neat water surface. Compared to the neat water SFG intensity in the hydrogen bonding region, the higher SFG response from the α-alumina (0001) surface may occur according to 2 possible scenarios (a nonresonant response scenario was tested and did not contribute to the increased 'effective' response). One is that the orientations of the structured water molecules are more ordered at the alumina surface than those of the air−water interface. Enhancement is observed in both the 3250 and 3450 cm^{-1} regions. However, the 3450 cm^{-1} region is more intense, not necessarily consistent with ordering of the surface water; however, interactions with the alumina surface hydroxyls may weaken the water−water hydrogen bonds, increasing the vibrational energy (frequency (cm^{-1})) of the molecules in the H-bonding network. Therefore, the water molecules could still be more highly aligned. This is consistent with an increase in the OH stretching region of H-bonded water. A second scenario is that the higher SFG intensity from the hydrated alumina surfaces can have contributions from the hydrogen bonded aluminol OH stretching, consistent with reported frequencies for more highly coordinated Al−O−H (*52*, *53*). Additional studies using D_2O instead of H_2O are needed to help distinguish between the two scenarios. These studies are currently underway.

Unlike the α-Al_2O_3 (0001) surface, a weaker SFG response in the hydrogen bonding region from the fused silica (amorphous) surface reveals the relatively hydrophobic nature of this surface as shown in Figure 5a. (Nonlinear Fresnel factors have been calculated for the alumina and silica surfaces and reveal that the silica surface gives a higher Fresnel factor.) There are numerous studies of water adsorption on silica surfaces using infrared adsorption in addition to many other methods (*14*, *15*, *20*). These results are not consistent with each other, especially in terms of the water coverage (*19*, *55*, *56*). The inconsistent data may be the result of differences in the materials used, sample pretreatment methods, experimental conditions (vacuum or ambient), and analytical methods.

In Figure 5a, at ambient conditions with 54% RH, the SFG spectrum of the air−silica interface reveals a weak hydrogen bonded OH stretch band, whereas a strong silanol OH stretching peak is observed around 3750 cm^{-1}. To ensure that the 3750 cm^{-1} peak was due to the free silianol OH stretch instead of other free OH stretches from adsorbed water molecules, an SFG spectrum was obtained at 0% RH as shown in Figure 5a. The SFG intensity of the 3750 cm^{-1} peak at 0% RH increases slightly compared to that of the 54% RH SFG spectrum. This indicates that the 3750 cm^{-1} peak is indeed due to the free silianol OH stretch. At 54% RH, the SFG spectrum suggests that water molecules may only cover a limited portion of the hydrated silica surface and that isolated silanol OH groups are present as the major surface species. While numerous infrared studies have observed the isolated silanol OH stretching frequency in the same spectral region (*10*−*16*), to our knowledge, this is the first published

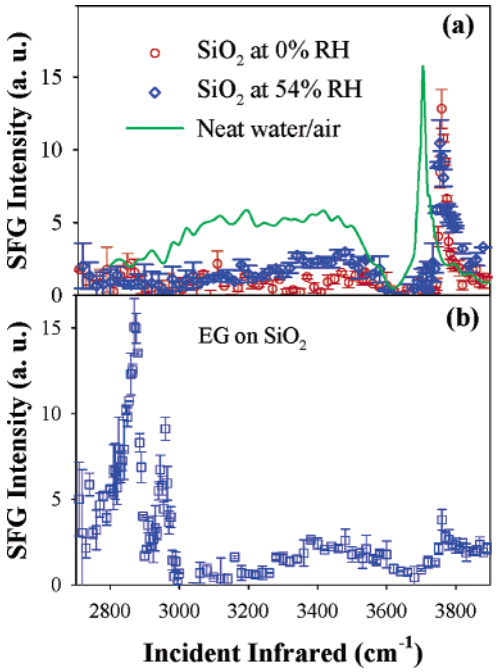

FIGURE 5. Sum frequency generation spectra of the silica surface (a) before and (b) after exposure to ethylene glycol vapor at 54% RH.

SFG spectra revealing the silanol OH from the air−silica interface, although solid−liquid SFG spectra of silica−water have been published by other groups (*38*, *57*).

The SFG spectra of ethylene glycol adsorbed on hydrated alumina and silica surfaces are shown in Figures 4 and 5b. The presence of the methylene CH stretching modes of EG molecules indicates the adsorption of EG molecules on both oxide surfaces. The slight decrease of the SFG intensity in the hydrogen bonded OH region on the α-Al_2O_3 surface (Figure 4) may suggest to a small extent, perturbation of the hydrogen bonding structures after adsorption of EG. (However, destructive interference with the CH modes may be the cause of this as fitting parameters can be forced to provide this change in spectral shape of the OH region.) The peak at ~3710 cm^{-1} remains unchanged, which suggests that this peak may indeed be the hydroxyl group (Al−O−H) on the α-Al_2O_3 surface as opposed to the free dangling OH of adsorbed water since the presence of EG molecules at the air−aqueous solution surface reduces the intensity of the free OH stretching as discussed above. Molecular dynamics calculations of water adsorption on the boehmite (010) surface indicate that water molecules do not cover the entire surface, moreover, adsorbed water forms island type multilayers, leaving a fraction of the aluminol OH groups exposed (personal communication with L. Criscenti, Sandia National Lab). One might expect the same results from the α-Al_2O_3 surface since both the hydroxylated α-Al_2O_3 surface and the boehmite surface are quite similar (boehmite is only slightly more hydrophilic than α-Al_2O_3). Therefore, it is possible that isolated α-Al_2O_3 hydroxyl groups will still exist without forming hydrogen bonds with surface water molecules under 54% RH at 296 K. If this is true, then EG is preferentially hydrogen bonding with the surface adsorbed water and not the isolated α-Al_2O_3 hydroxyl groups. This is further elucidated following the continuing discussions on the SFG spectrum changes in the CH stretching region.

As shown in Figure 5b, after adsorption of EG molecules on the SiO_2 surface, the isolated silanol OH stretching peak is suppressed to a great extent relative to this peak observed from the SiO_2 surface at 54% RH (Figure 5a). In addition, there are no EG free OH peaks observed. These observations suggest that EG molecules form hydrogen bonds with the

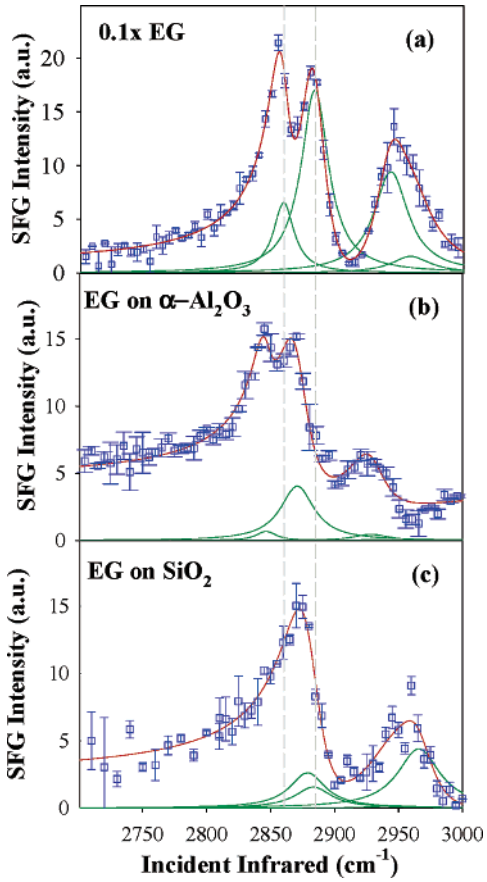

FIGURE 6. Sum frequency generation spectra in the C−H stretching region of ethylene glycol molecules (a) at the air−aqueous interface, (b) adsorbed on the alumina surface, and (c) adsorbed on the silica surface. Ethylene glycol at the air−aqueous solution interface is plotted in (a) for comparison purposes. The red lines are spectroscopic fits, and the dark green lines are the component peaks. (The nonresonant SFG fitting parameters are different for all 3 spectra; component peak phases are all positive.)

surface silanol groups, and EG can act as a hydrogen acceptor and a hydrogen donor to the other acceptors (surface silanol groups, water molecules, or other EG molecules). These results are in agreement with the FT-IR studies which concluded that hydrogen bond formation between the adsorbate molecules and the hydrogen atoms of the silanol groups on the silica surface plays a major role in adsorption of molecules from the vapor state (*15*, *20*).

It is difficult to analyze the hydrogen bonding structure based on the OH stretching region alone since there is a lack of informative features in this region due to the broadness of the hydrogen bonded OH stretching bands. In addition, the oxide surface under ambient conditions with the presence of water vapor and organic molecules containing hydroxyl groups is complex. However, the spectroscopic features in the CH stretching region can give key information about the hydrogen bonding structure since changing the local hydrogen bonding environment will affect the frequencies of the CH stretching modes. Figure 6(a−c) compares the SFG spectra and relative CH stretching frequencies of the 0.1x EG solution, the EG adsorbed on the alumina surface (EG_{Al}), and the SiO_2 (EG_{Si}) surface. The CH_2−SS peaks of the SFG spectrum of EG_{Al} (Figure 6b) resembles that of the aqueous EG solution at low concentration (≤ 0.1x in Figure 2) which reveals a splitting feature at ∼2855 and ∼2880 cm^{-1}. In contrast, the CH_2−SS peak of the SFG spectrum of EG_{Si} (Figure 6c) is similar to that of the aqueous EG solution at higher concentrations (> 0.1x in Figure 2). This is consistent with the discussions above that suggest that the EG molecule adsorbs on the relatively hydrophilic α-Al_2O_3 (0001) surface (*58*) by forming hydrogen bonds with adsorbed water molecules and that the EG molecule forms hydrogen bonds with silanol OH groups on the relatively hydrophobic SiO_2 surface. (At 54% RH, the SiO_2 surface does not have as many water molecules adsorbed to its surface as that of the α-Al_2O_3 surface as indicated by Figures 4a and 5a.) As shown in Figure 6(a−c), the CH_2−SS peak positions of the SFG spectrum of EG_{Al} are shifted ∼15 cm^{-1} to lower frequency relative to that of the aqueous EG solutions (Figure 2). The red shift of the CH_2−SS peaks suggests that hydrogen bonding between the adsorbed water molecules and the EG molecules is relatively weak compared to that at the aqueous EG−air interface, consistent with cluster studies (*51*). This was further tested by the complete desorption of EG (no CH stretching SFG signal detected) after rinsing EG adsorbed α-Al_2O_3 (0001) with organic free deionized water for 5 min. The hydrogen bonding strength can therefore be described as weakly physisorbed. There is a convolution of the ∼2855 cm^{-1} and the ∼2880 cm^{-1} CH_2−SS peaks in the EG_{Si} spectrum, suggesting one continuous distribution of EG comformers and orientations as opposed to the bimodal distribution (CH_2−SS peak splitting) observed for the low EG mole fractions at the liquid surface as well as at the surface of the alumina. In addition, there is no SFG signal in the EG CH stretching region after rinsing EG adsorbed SiO_2 for 5 min with water. This also suggests that the hydrogen bonds between EG molecules and silanol OH group are also weak relative to that at the aqueous EG−air interface (i.e. weakly physisorbed). However, the observed shifts, splitting and lack of splitting from the different interfaces clearly indicate that the adsorbed EG molecules interact in different ways at the two different oxide surfaces. Interestingly, the EG adsorption on the alumina surface exhibits splitting similar to the low concentration EG solution surface, yet the silica surface does not allow the EG to preferentially reorient. In addition, the surface hydrophilic versus hydrophobic properties seem to strongly influence the ability of EG to reorient itself.

Acknowledgments

We acknowledge the U.S. Department of Energy (DOE-BES Geosciences DE-FG02-04ER15495) in addition to the NSF Ohio State Environmental Molecular Science Institute (CHE-0089147) for the funding of this project.

Supporting Information Available

All the SFG peak fitting parameters and infrared and Raman spectra of ethylene glycol. This material is available free of charge via the Internet at http://pubs.acs.org.

Literature Cited

(1) Sparks, D. L. *Environmental Soil Chemistry*, 2nd ed.; Academic Press: San Diego, CA, 2003.
(2) Stumm, W.; Morgan, J. J. *Aquatic Chemistry*, 3rd ed.; John Wiley & Sons: New York, 1996.
(3) Usher, C. R.; Michel, A. E.; Grassian, V. H. Reactions on Mineral Dust. *Chem. Rev.* **2003**, *103* (12), 4883.
(4) Al-Abadleh, H. A.; Grassian, V. H. Oxide Surfaces as Environmental Interfaces. *Surf. Sci. Rep.* **2003**, *52* (3−4), 63.
(5) *Minerals in Soil Environments. SSSA Book Ser. 1*; Dixon, J. B., Weed, S. B., Eds.; Soil Sci. Soc. Am.: Madison, WI, 1989.
(6) El Rassi, Z.; Gonnet, C.; Rocca, J. L. Chromatographic Studies of the Influence of Water and Thermal Treatment on the Activity of Silica Gel. *J. Chromatogr.* **1976**, *125*, 179.
(7) Unger, K. K. *Porous Silica*; Elsevier: Amsterdam, 1979.
(8) Eng, P. J.; Trainor, T. P.; Brown, G. E., Jr.; Waychunas, G. A.; Newville, M.; Sutton, S. R.; Rivers, M. L. Structure of the Hydrated α-Al_2O_3 (0001) Surface. *Science* **2000**, *288* (5468), 1029.
(9) Hass, K. C.; Schneider, W. F.; Curioni, A.; Andreoni, W. The Chemistry of Water on Alumina Surfaces: Reaction Dynamics from First Principles. *Science* **1998**, *282* (5387), 265.
(10) Burneau, A.; Barres, O.; Gallas, J. P.; Lavalley, J. C. Comparative Study of the Surface Hydroxyl Groups of Fumed and Precipitated

Silicas. 2. Characterization by Infrared Spectroscopy of the Interactions with Water. *Langmuir* **1990**, *6* (8), 1364.
(11) Burneau, A.; Barres, O.; Vidal, A.; Balard, H.; Ligner, G.; Papirer, E. Comparative Study of the Surface Hydroxyl Groups of Fumed and Precipitated Silicas. 3. Drift Characterization of Grafted N−Hexadecyl Chains. *Langmuir* **1990**, *6* (8), 1389.
(12) McFarlan, A. J.; Morrow, B. A. Infrared Evidence for Two Isolated Silanol Species on Activated Silicas. *J. Phys. Chem.* **1991**, *95*, 5388.
(13) Morrow, B. A.; McFarlan, A. J. Surface Vibrational Modes of Silanol Groups on Silica. *J. Phys. Chem.* **1992**, *96*, 1395.
(14) Morrow, B. A.; Gay, I. D. Infrared and NMR Characterization of the Silica Surface. In *Adsorption on Silica Surface*; Papirer, E., Ed.; Marcel Dekker: New York, 2000.
(15) Iler, R. K. *The Chemistry of Silica: Solubility, Polymerization, Colloid and Surface Properties, and Biochemistry*; Wiley-Interscience Publication, John Wiley & Sons: New York, 1979.
(16) Sneh, O.; George, S. M. Thermal Stability of Hydroxyl Groups on a Well-Defined Silica Surface. *J. Phys. Chem.* **1995**, *99*, 4639.
(17) de Leeuw, N. H.; Higgins, F. M.; Parker, S. C. Modeling the Surface Structure and Stability of α-Quartz. *J. Phys. Chem. B* **1999**, *103*, 1270.
(18) Al-Abadleh, H. A.; Grassian, V. H. FT-IR Study of Water Adsorption on Aluminum Oxide Surfaces. *Langmuir* **2003**, *19* (2), 341.
(19) Sneh, O.; Cameron, M. A.; George, S. M. Adsorption and Desorption Kinetics of H_2O on a Fully Hydroxylated SiO_2 Surface. *Surf. Sci.* **1996**, *364* (1), 61.
(20) Davydov, V. Y. Adsorption on Silica Surfaces. In *Adsorption on Silica Surfaces*; Papirer, E., Ed.; Marcel Dekker: New York, 2000; p 63.
(21) Natal-Santiago, M. A.; Hill, J. M.; Dumesic, J. A. Studies of the Adsorption of Acetaldehyde, Methyl Acetate, Ethyl Acetate, and Methyl Trifluoacetate on Silica. *J. Mol. Catal. A: Chem.* **1999**, *140*, 199.
(22) Morrow, B. A.; McFarlan, A. J. Chemical Reactions at Silica Surfaces. *J. Non-Cryst. Solids* **1990**, *120* (1−3), 61.
(23) Zaki, M. I.; Hasan, M. A.; Al-Sagheer, F. A.; Pasupulety, L. In Situ FTIR Spectra of Pyridine Adsorbed on SiO_2−Al_2O_3, TiO_2, ZrO_2 and CeO_2: General Considerations for the Identification of Acid Sites on Surfaces of Finely Divided Metal Oxides. *Colloid Surf.* **2001**, *190*, 261.
(24) Dines, T. J.; MacGregor, L. D.; Rochester, C. H. Adsorption of 2-Chloropyridine on Oxide—an Infrared Spectroscopic Study. *Spectrochim. Acta, Part A* **2003**, *59*, 3205.
(25) Hair, M. L.; Hertl, W. Adsorption on Hydroxylated Silica Surface. *J. Phys. Chem.* **1969**, *73*, 4269.
(26) Inaki, Y.; Yoshida, H.; Yoshida, T.; Hattori, T. Active Sites on Mesoporous and Amorphous Silica Materials and Their Photocatalytic Activity: An Investigation by FTIR, ESR, VUV−UV and Photoluminescence Spectroscopies. *J. Phys. Chem. B* **2002**, *106*, 9098.
(27) Goss, K.-U.; Schwarzenbach, R. P. Adsorption of a Diverse Set of Organic Vapors on Quartz, $CaCO_3$, and α-Al_2O_3 at Different Relative Humidities. *J. Colloid Interface Sci.* **2002**, *252* (1), 31.
(28) Goss, K.-U.; Eisenreich, S. J. Adsorption of VOCs from the Gas Phase to Different Minerals and a Mineral Mixture. *Environ. Sci. Technol.* **1996**, *30* (7), 2135.
(29) Goss, K. U. Effects of Temperature and Relative Humidity on the Sorption of Organic Vapors on Quartz Sand. *Environ. Sci. Technol.* **1992**, *26* (11), 2287.
(30) Goss, K.-U.; Schwarzenbach, R. P. Quantification of the Effect of Humidity on the Gas/Mineral Oxide and Gas/Salt Adsorption of Organic Compounds. *Environ. Sci. Technol.* **1999**, *33* (22), 4073.
(31) Goss, L. M.; Sharpe, S. W.; Blake, T. A.; Vaida, V.; Brault, J. W. Direct Absorption Spectroscopy of Water Clusters. *J. Phys. Chem. A* **1999**, *103*, 8620.
(32) Ong, S. K.; Lion, L. W. Mechanisms for Trichloroethylene Vapor Sorption onto Soil Minerals. *J. Environ. Qual.* **1991**, *20* (1), 180.
(33) Petersen, L. W.; Moldrup, P.; El-Farhan, Y. H.; Jacobsen, O. H.; Yamaguchi, T.; Rolston, D. E. The Effect of Moisture and Soil Texture on the Adsorption of Organic Vapors. *J. Environ. Qual.* **1995**, *24* (4), 752.
(34) Brown, G. E., Jr.; Sturchio, N. C. An Overview of Synchrontron Radiation Application to Low-Temperature Geochemistry and Environmental Science. *Rev. Min. Geochem.* **2002**, *49*, 1.
(35) Brown, G. E., Jr.; Henrich, V. E.; Casey, W. H.; Clark, D. L.; Eggleston, C.; Felmy, A.; Goodman, D. W.; Graetzel, M.; Maciel, G.; McCarthy, M. I.; Nealson, K. H.; Sverjensky, D. A.; Toney, M. F.; Zachara, J. M. Metal Oxide Surfaces and Their Interactions with Aqueous Solutions and Microbial Organisms. *Chem. Rev.* **1999**, *99* (9), 77.
(36) Shen, Y. R. *The Principles of Nonlinear Optics*, 1st ed.; John Wiley & Sons: New York, 1984.
(37) Bloembergen, N.; Pershan, P. S. Light Waves at the Boundary of Nonlinear Media. *Phys. Rev.* **1962**, *128* (2), 606.
(38) Miranda, P. B.; Shen, Y. R. Liquid Interfaces: A Study by Sum-Frequency Vibrational Spectroscopy. *J. Phys. Chem. B* **1999**, *103*, 3292.
(39) Hirose, C.; Akamatsu, N.; Domen, K. Formulas for the Analysis of the Surface SFG Spectrum and Transformation Coefficients of Cartesian SFG Tensor Components. *Appl. Spectrosc.* **1992**, *46* (6), 1051.
(40) Moad, A. J.; Simpson, G. J. A Unified Treatment of Selection Rules and Symmetry Relations for Sum-Frequency and Second Harmonic Spectroscopies. *J. Phys. Chem. B* **2004**, *108*, 3548.
(41) Hommel, E.; Merle, J.; Ma, G.; Hadad, C.; Allen, H. C. Spectroscopic and Computational Studies of Aqueous Ethylene Glycol Solution Surfaces. **2004**, submitted 6−04.
(42) Lu, R.; Gan, W.; Wu, B.-H.; Chen, H.; Wang, H.-F. Vibrational Polarization Spectroscopy of CH Stretching Modes of the Methylene Group at the Vapor/Liquid Interfaces with Sum Frequency Generation. *J. Phys. Chem. B* **2004**, *108*, 7297.
(43) Chaudhari, A.; Lee, S.-L. A Computational Study of Microsolvation Effect on Ethylene Glycol by Density Functional Method. *J. Chem. Phys.* **2004**, *120* (16), 7464.
(44) Nagy, P. I.; Dunn, W. J., III.; Alagona, G.; Ghio, C. Theoretical Calculations on 1,2-Ethanediol. 2. Equilibrium of the Gauche Conformers with and without an Intramolecular Hydrogen Bond in Aqueous Solution. *J. Am. Chem. Soc.* **1992**, *114* (12), 4752.
(45) Cramer, C. J.; Truhlar, D. G. Quantum Chemical Conformational Analysis of 1,2-Ethanediol: Correlation and Solvation Effects on the Tendency to Form Internal Hydrogen Bonds in the Gas Phase in Aqueous Solution. *J. Am. Chem. Soc.* **1994**, *116*, 3892.
(46) Hommel, E. L.; Allen, H. C. The Air−Liquid Interface of Benzene, Toluene, M-Xylene, and Mesitylene: A Sum Frequency, Raman, and Infrared Spectroscopic Study. *Analyst* **2003**, *128*, 750.
(47) Szymanski, H. A. *Interpreted Infrared Spectra*; Plenum Press Data Division: New York, 1966; Vol. 2.
(48) Krueger, P. J.; Mettee, H. D. Spectroscopic Studies of Alcohols, Part VII. Intramolecular Hydrogen Bonds in Ethylene Glycol and 2-Methoxyethanol. *J. Mol. Spectrosc.* **1965**, *18*, 131.
(49) Du, Q.; Superfine, R.; Freysz, E.; Shen, Y. R. Vibrational Spectroscopy of Water at the Vapor/Water Interface. *Phys. Rev. Lett.* **1993**, *70* (15), 2313.
(50) Stanners, C. D.; Du, Q.; Chin, R. P.; Cremer, P.; Somorjai, G. A.; Shen, Y. R. Polar Ordering at the Liquid−Vapor Interface of N−Alcohols (C1−C8). *Chem. Phys. Lett.* **1995**, *232* (4), 407.
(51) Ma, G.; Allen, H. C. Surface Studies of Aqueous Methanol Solutions by Vibrational Broad Bandwidth Sum Frequency Generation Spectroscopy. *J. Phys. Chem. B* **2003**, *107*, 6343.
(52) Knozinger, H.; Ratnasamy, O. Catalytic Aluminas: Surface Models and Characterization of Surfaces Sites. *Catal. Rev.-Sci. Eng.* **1978**, *17*, 31.
(53) Mawhinney, D. B.; Rossin, J. A.; Gerhart, K.; Yates, J. T., Jr. Infrared Spectroscopic Study of Surface Diffusion to Surface Hydroxyl Groups on Al_2O_3: 2-Chloroethylethyl Sulfide Adsorption Site Selection. *Langmuir* **2000**, *16*, 2237.
(54) Hass, K. C.; Schneider, F. W.; Curioni, A.; Andreoni, W. First-Principles Molecular Dynamics Simulations of H_2O on α-Al_2O_3 (0001). *J. Phys. Chem. B* **2000**, *104*, 5527.
(55) de la Caillerie, J.-B. d. E.; Aimeur, M. R.; Kortobi, Y. E.; Legrand, A. P. Water Adsorption on Pyrogenic Silica Followed by ^1H MAS NMR. *J. Colloid Interface Sci.* **1997**, *194*, 434.
(56) Zhuravlev, L. T. The Surface Chemistry of Amorphous Silica. Zhuravlev Model. *Colloid Surf.* **2000**, *173*, 1.
(57) Kim, J.; Kim, G.; Cremer, P. S. Investigations of Polyelectrolyte Adsorption at the Solid/Liquid Interface by Sum Frequency Spectroscopy: Evidence for Long-Range Macromolecular Alignment at Highly Charged Quartz/Water Interfaces. *J. Am. Chem. Soc.* **2002**, *124*, 8751.
(58) Chattoraj, D. K.; Birdi, K. S. *Adsorption and Gibbs' Surface Excess*; Plenum Press: New York, 1984.

Received for review June 21, 2004. Revised manuscript received September 17, 2004. Accepted September 27, 2004.

ES049066A